Motionally Restricted Tryptophan Environments at the Peptide–Lipid Interface of Gramicidin Channels†

Sushmita Mukherjee and Amitabha Chattopadhyay*

Centre for Cellular and Molecular Biology, Uppal Road, Hyderabad 500 007, India

Received September 14, 1993; Revised Manuscript Received January 31, 1994®

ABSTRACT: The tryptophans in the gramicidin channel play a crucial role in the organization and function of the channel. The localization and dynamics of these tryptophans have been studied using fluorescence spectroscopy, especially utilizing environment-induced effects on the rates of solvent relaxation around these residues in membranes. When incorporated into model membranes of dioleoyl-*sn*-glycero-3-phosphocholine (DOPC), the tryptophans in the gramicidin channel exhibit a red edge excitation shift (REES) of 6 nm. In addition, fluorescence polarization shows both excitation and emission wavelength dependence. Fluorescence lifetime analysis shows a biexponential decay, corresponding to a short- and a long-lifetime component. The mean lifetime was found to be dependent on both excitation and emission wavelengths. Analysis of time-resolved emission spectra (TRES) shows a heterogeneous environment for the tryptophans consistent with the lifetime information. Taken together, these observations point out the motional restriction experienced by the tryptophans in the gramicidin channel. This is consistent with other studies in which such restrictions are thought to be imposed due to hydrogen bonding between the indole rings of the tryptophans and the neighboring lipid carbonyls. The significance of such organization in terms of functioning of the channel is brought out by the fact that substitution, photodamage, or chemical modification of these tryptophans is known to give rise to channels with altered conformation and reduced conductivity.

Maintenance of appropriate ion balance inside and outside a biological membrane is crucial for cellular integrity and function. The concept of specific ionic pathways in membranes has now evolved to the point where selectivity can be addressed in terms of the three-dimensional conformation of the primary sequence of ion channel proteins (Guy, 1988; Andersen & Koeppe, 1992). The elucidation of ion channel function could thus be viewed as a more general problem in membrane structural biology—that of modulation of the structure, organization, and dynamics of the ion channel by its immediate membrane milieu (Andersen *et al.*, 1992).

The linear gramicidins are a family of prototypical channel-formers and are extensively used to study organization, dynamics, and function of membrane-spanning channels [for reviews on gramicidin, see Andersen (1984), Cornell (1987), Wallace (1990), Killian (1992), and Busath (1993)]. Due to their small size, ready availability, and the relative ease with which chemical modifications can be performed, gramicidins serve as excellent models for transmembrane channels. Gramicidins are linear pentadecapeptide antibiotics with a molecular weight of ~1900. They are produced by the bacterium *Bacillus brevis*, and consist of alternating L- and D-amino acids (Sarges & Witkop, 1965; Rinehart *et al.*, 1977). The natural mixture of gramicidins, often denoted as gramicidin A′ or gramicidin D, consists of ~85% of gramicidin A, which has four tryptophan residues at positions 9, 11, 13, and 15. Gramicidin A′ is readily available commercially and is fluorescent, due to the presence of the tryptophan residues. It has one of the most hydrophobic sequences known (Segrest & Feldmann, 1974), and has been widely used as a model peptide for membrane-spanning regions of intrinsic membrane proteins (Chapman *et al.*, 1977; Weidekamm *et al.*, 1977; Rice & Oldfield, 1979; Susi *et al.*, 1979).

Gramicidin forms channels in lipid membranes which are selective for monovalent cations (Hladky & Haydon, 1972; Finkelstein & Andersen, 1981; Andersen, 1984). The peptide dimerizes spontaneously in lipid bilayers to form single-file cation channels. While the interior of the channel is thought to be formed by the peptide backbone, the side chains project outward and modulate the channel conductance.

The presence of alternating D- and L-amino acids in gramicidin produces secondary structures not generally encountered in the case of peptides and proteins which contain only L-amino acids. Several structural models exist in the literature for gramicidin incorporated into membranes (Urry, 1971; Urry *et al.*, 1971; Ramachandran & Chandrasekaran, 1972; Veatch & Blout, 1974; Wallace, 1986). It is generally believed (Urry *et al.*, 1971; Wallace, 1990; Killian, 1992) that in its membrane-bound form, gramicidin exists as a head-to-head (amino terminal-to-amino terminal) single-stranded $\beta^{6.3}$-helical dimer, originally termed the $\pi^{6}_{L,D}$ helix, which is stabilized by six hydrogen bonds and forms a continuous water-filled channel. According to this model, there are 6.3 residues per turn and a central hole about 4 Å in diameter. The dimer would be about 25–30 Å in length, which approximates the size necessary to span a lipid bilayer. The carboxy termini in such a conformation are exposed to the membrane surface, while the amino termini are buried in the lipid bilayer.

Since the tryptophans in gramicidin are all localized near its C-terminus (Feigenson *et al.*, 1977; Haigh *et al.*, 1979), the preference for the $\beta^{6.3}$-helical conformation in the membrane environment has been suggested to be due to a preferred orientation of the tryptophans near the lipid–water interface. This is supported by several examples of membrane proteins in which tryptophans have been found to be preferentially localized in this region (Jacobs & White, 1989;

† This work was supported by the Council of Scientific and Industrial Research, Government of India. S.M. was awarded a Junior Research Fellowship by the University Grants Commission.

* Address correspondence to this author. Fax: +91-40-851195.

® Abstract published in *Advance ACS Abstracts,* April 1, 1994.

0006-2960/94/0433-5089$04.50/0

Michel & Deisenhofer, 1990; Meers, 1990; Chattopadhyay & McNamee, 1991; Weiss *et al.*, 1991; Schiffer *et al.*, 1992). This preferred localization of the tryptophan residues near the lipid–water interface has been ascribed to the ability of the tryptophan –NH groups to form hydrogen bonds with the hydrogen bond acceptors near the lipid head groups, one of the strongest candidates for such acceptors being the lipid carbonyls (Ippolito *et al.*, 1990). Interfacial water molecules present near the lipid head-group region also form a distinct class of possible hydrogen bond acceptors. The proposition that the tryptophan residues of membrane-bound gramicidin channels are indeed hydrogen-bonded to the neighboring hydrogen bond acceptors is further supported by the fact that for the gramicidin chemical mutant in which all four tryptophan residues are replaced by phenylalanines, which are more hydrophobic and cannot act as hydrogen bond donors, the peptide seems to preferentially adopt the alternate antiparallel double-stranded helical dimer conformation (Bano *et al.*, 1992), and exhibits drastically reduced channel activity (Becker *et al.*, 1991; Fonseca *et al.*, 1992). Also in line with the above observations is the fact that a change in permeability characteristics of the gramicidin channels occurs due to weaker hydrogen bonding while ether lipids are used instead of ester lipids (Meulendijks *et al.*, 1989).

In this paper, we have utilized the phenomenon of red edge excitation shift (REES)[1] in particular, and the relatively slow rates of solvent dipole reorientation around the excited-state tryptophans of gramicidin in general, in order to study the organization and dynamics of the functionally important tryptophan residues at the peptide–lipid interface in the gramicidin channel. A shift in the wavelength of maximum fluorescence emission toward higher wavelengths, caused by a shift in the excitation wavelength toward the red edge of the absorption band, is termed the red edge excitation shift (REES). This effect is mostly observed with polar fluorophores in motionally restricted media such as very viscous solutions or condensed phases. The origin of the red edge effect lies in the change in fluorophore–solvent interactions in the ground and excited states, brought about by a change in the dipole moment of the fluorophore upon excitation, and the rate at which solvent molecules reorient around the excited-state fluorophore (Galley & Purkey, 1970; Demchenko, 1982, 1988; Lakowicz & Keating-Nakamoto, 1984; Chattopadhyay & Mukherjee, 1993). We have recently shown that REES serves as a powerful tool to monitor the organization and dynamics of membrane-bound probes (Chatttopadhyay, 1991; Chattopadhyay & Mukherjee, 1993; Chattopadhyay & Rukmini, 1993).

Our present results confirm the restricted environment experienced by the functionally important tryptophan residues at the peptide–lipid interface of the gramicidin channel possibly due to hydrogen bonding interactions with neighboring groups. Furthermore, our time-resolved fluorescence studies indicate that the channel tryptophans can be grouped into at least two classes experiencing very different microenvironments.

MATERIALS AND METHODS

DOPC was purchased from Avanti Polar Lipids (Birmingham, AL). Gramicidin A′ (from *Bacillus brevis*) and DMPC were purchased from Sigma Chemical Co. (St. Louis, MO). Gramicidin A′, as obtained, is a mixture of gramicidins A, B, and C. Lipids were checked for purity by TLC on silica gel plates in chloroform/methanol/water (65:35:5, v/v/v). DOPC gave one spot with a phosphate-sensitive spray and subsequent charring (Dittmer & Lester, 1964). Lipid concentration was determined by phosphate assay subsequent to total digestion by perchloric acid (McClare, 1971). DMPC was used as a standard to assess lipid digestion. Solvents used were of spectroscopic grade. Water was purified through a Millipore (Bedford, MA) Milli-Q system and used throughout.

All experiments were done using unilamellar vesicles (ULV) of DOPC containing 1% (mol/mol) gramicidin A′. In general, 1280 nmol of DOPC in chloroform was mixed with 12.8 nmol of gramicidin in methanol. A few drops of chloroform were added and mixed well, and the samples were dried under a stream of nitrogen while warming gently (~35 °C). After further drying under a high vacuum for at least 3 h, 3 mL of 10 mM sodium phosphate/150 mM sodium chloride buffer, pH 7.0–7.2, was added, and each sample was vortexed for 3 min to disperse the lipids. The lipid dispersions so obtained were sonicated for 10 min (in bursts of 1 min, followed by immediate cooling in ice) using a Branson B-30 sonifier. The samples were then centrifuged at 15 000 rpm for 20 min to remove titanium particles and incubated overnight at 65 °C with continuous stirring in order to induce the channel conformation (Lograsso *et al.*, 1988; Killian *et al.*, 1988). Background samples were prepared the same way except that gramicidin was omitted. All experiments were done with multiple sets of samples. The spectral shifts obtained with different sets of samples were identical in most cases. In other cases, the values were within ±1 nm of the ones reported. All experiments were done at 23 °C.

Steady-state fluorescence measurements were performed with a Hitachi F-4010 steady-state spectrofluorometer using 1-cm path-length quartz cuvettes. Excitation and emission slits with a nominal band-pass of 5 nm were used. Background intensities of samples in which gramicidin was omitted were subtracted from each sample spectrum to cancel out any contribution due to the solvent Raman peak and other scattering artifacts. Fluorescence polarization measurements were performed using a Hitachi polarization accessory. Polarization values were calculated from the equation (Chen & Bowman, 1965):

$$P = \frac{I_{VV} - GI_{VH}}{I_{VV} + GI_{VH}} \quad (1)$$

where I_{VV} and I_{VH} are the measured fluorescence intensities with the excitation polarizer vertically oriented and the emission polarizer vertically and horizontally oriented, respectively. G is the grating correction factor and is equal to I_{HV}/I_{HH}.

Fluorescence lifetimes were calculated from time-resolved fluorescence intensity decays using a Photon Technology International (London, Western Ontario, Canada) LS-100 luminescence spectrophotometer operated in the time-correlated single photon counting mode. This machine uses a thyratron-gated nanosecond flash lamp filled with nitrogen as the plasma gas (15 ± 1 in. of mercury vacuum) and runs at 22–25 kHz. Lamp profiles were measured at the excitation wavelength using Ludox as the scatterer. To optimize the signal to noise ratio, 10 000 photon counts were collected in the peak channel. All experiments were performed using slits with a nominal band-pass of 8 nm or less. The sample and the scatterer were alternated after every 10% acquisition to ensure compensation for shape and timing drifts occurring

[1] Abbreviations: DMPC, dimyristoyl-*sn*-glycero-3-phosphocholine; DOPC, dioleoyl-*sn*-glycero-3-phosphocholine; NBD, 7-nitro-2,1,3-benzoxadiazol-4-yl; NBD-PE, *N*-(7-nitro-2,1,3-benzoxadiazol-4-yl)dipalmitoyl-*sn*-glycero-3-phosphoethanolamine; NMR, nuclear magnetic resonance; REES, red edge excitation shift; SDS, sodium dodecyl sulfate; TLC, thin-layer chromatography; TRES, time-resolved emission spectra; ULV, unilamellar vesicle.

during the period of data collection. The data stored in a multichannel analyzer were routinely transferred to an IBM PC/AT computer for analysis. Intensity decay curves were fitted as a sum of exponential terms:

$$F(t) = \sum_i \alpha_i \exp(-t/\tau_i) \quad (2)$$

where α_i is a preexponential factor representing the fractional contribution to the time-resolved decay of the component with a lifetime τ_i. The decay parameters were recovered using a nonlinear least-squares iterative fitting procedure based on the Marquardt algorithm (Bevington, 1969). The program also includes statistical and plotting subroutine packages (O'Connor & Phillips, 1984). The goodness of fit of a given set of observed data and the chosen function was evaluated by the reduced χ^2 ratio, the weighted residuals (Lampert *et al.*, 1983), the autocorrelation function of the weighted residuals (Grinvald & Steinberg, 1974), the runs test (Hamburg, 1985), and the Durbin–Watson parameters (Durbin & Watson, 1950). A fit was considered acceptable when plots of the weighted residuals and the autocorrelation function showed random deviation about zero with a χ^2 value not more than 1.9. Mean (average) lifetimes, $\langle\tau\rangle$, for biexponential decays of fluorescence were calculated from the decay times and preexponential factors using the equation (Lakowicz, 1983):

$$\langle\tau\rangle = \frac{\alpha_1\tau_1^2 + \alpha_2\tau_2^2}{\alpha_1\tau_1 + \alpha_2\tau_2} \quad (3)$$

Fractional intensities corresponding to each lifetime component were calculated using (Lakowicz, 1983)

$$f_i = \frac{\alpha_i\tau_i}{\sum_i \alpha_i\tau_i} \quad (4)$$

In order to obtain the time-resolved emission spectra (TRES), a series of fluorescence decays were acquired over a range of emission wavelengths (310–350 nm), using a constant excitation wavelength of 297 nm. All the decay curves were then individually fitted as a sum of exponential terms using the Marquardt algorithm as discussed above. The net result of such an analysis was a set of deconvoluted intensity decays at various emission wavelengths. This set of deconvoluted decays was then used to reconstruct a pseudo-three-dimensional TRES plot after renormalizing the intensities of the individual curves to that of the integrated emission intensity. This method has the advantage that convolution distortion is avoided because each curve is individually deconvoluted before the construction of the final TRES plot. The final TRES plot has an emission wavelength axis in nanometers, a time axis in nanoseconds, and a fluorescence intensity axis (O'Connor & Phillips, 1984).

RESULTS

The shift in the maxima of fluorescence emission[2] of the tryptophan residues of gramicidin A′ in DOPC vesicles as a function of excitation wavelength is shown in Figure 1. As the excitation wavelength is changed from 280 to 310 nm, the emission maximum is shifted from 331 to 337 nm, which corresponds to a REES of 6 nm. It is possible that there could be further red shift when gramicidin is excited beyond 310 nm. We found it difficult to work in this wavelength range because of the very low signal to noise ratio and artifacts due to the Raman peak that remained even after background subtraction. Observation of such a shift in the wavelength of maximum emission with a change in the excitation wavelength implies that the tryptophan residues of gramicidin channels are in an environment where their mobility is considerably reduced. Since the average location of the tryptophan residues of gramicidin channels is at the lipid–water interface (Killian, 1992), estimated to be ~14 Å from the center of the bilayer (Boni *et al.*, 1986), such a result would directly imply that this region of the membrane offers considerable restriction to the reorientational motion of the solvent dipoles around the excited-state fluorophore. This is in agreement with our previous observation that the NBD group of NBD-PE, which is located at a similar position in the DOPC bilayer (Chattopadhyay, 1990), also experiences a considerable restriction to its mobility from the surrounding membrane environment (Chattopadhyay & Mukherjee, 1993). Gramicidin A′ is a multi-tryptophan peptide, and thus the red edge shift, in the strictest sense, is only indicative of the average environment experienced by the tryptophans.

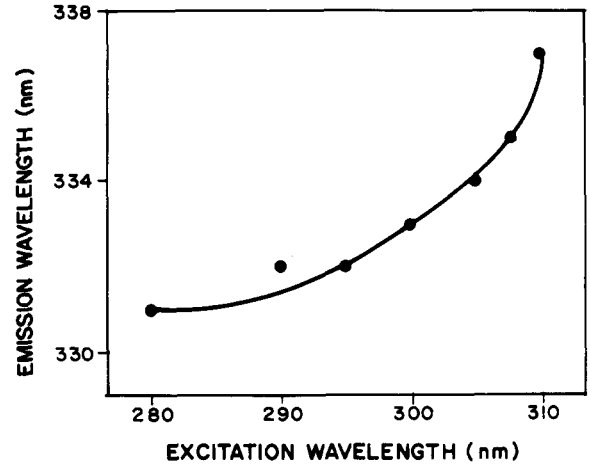

FIGURE 1: Effect of changing excitation wavelength on the wavelength of maximum emission for gramicidin A′ in DOPC vesicles. Fluorophore to lipid ratio was 1:100 (mol/mol). See Materials and Methods for other details.

In addition to the shift in the emission maximum on red edge excitation, fluorescence polarization is also known to be dependent on the excitation wavelength in viscous media (Weber, 1960a,b; Valeur & Weber, 1977, 1978; Lakowicz, 1984; Chattopadhyay & Mukherjee, 1993; Chattopadhyay & Rukmini, 1993). Due to strong dipolar interactions with the surrounding solvent molecules, there is a decreased rotational rate of the fluorophore in the relaxed state. On red edge excitation, a selective excitation of this subclass of fluorophores occurs. Because of strong interactions with the polar solvent molecules in the excited state, one may expect these "solvent-relaxed" fluorophores to rotate more slowly, thereby increasing the polarization (Lakowicz, 1984).

The excitation polarization spectra (*i.e.*, a plot of steady-state polarization *vs* excitation wavelength) of gramicidin A′ in model membranes of DOPC, and in methanol, are shown in Figure 2. The polarization of gramicidin in methanol remains essentially invariant over the range of excitation wavelengths. On the other hand, polarizations in the membrane change upon altering the excitation wavelength, with a sharp increase occurring toward the red edge of the

[2] We have used the term maximum of fluorescence emission in a somewhat wider sense here. In every case, we have monitored the wavelength corresponding to maximum fluorescence intensity, as well as the center of mass of the fluorescence emission. In most cases, both these methods yielded the same wavelength. In cases where minor discrepancies were found, the center of mass of emission has been reported as the fluorescence maximum.

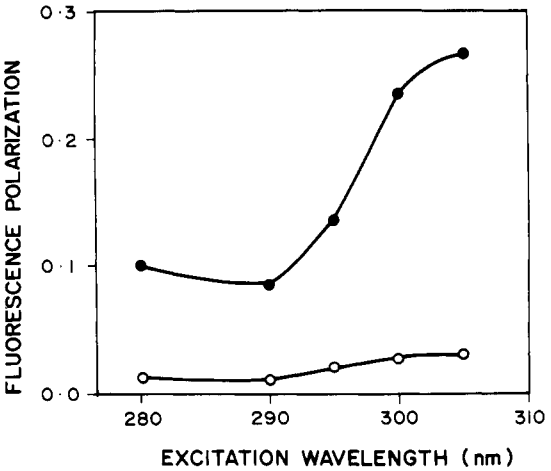

FIGURE 2: Fluorescence polarization of gramicidin A′ as a function of excitation wavelength in methanol (○) and in DOPC vesicles (●). Polarization values were recorded at 331 nm. Fluorophore to lipid ratio was 1:100 (mol/mol) in DOPC vesicles. Concentration of gramicidin A′ in methanol was 4.3 μM. See Materials and Methods for other details.

absorption band. Such an increase in polarization upon red edge excitation for peptides and proteins containing tryptophans as well as other aromatic fluorophores, especially in media of reduced mobility such as propylene glycol at low temperatures, has been reported before (Weber, 1960b; Valeur & Weber, 1978). This reinforces our previous conclusion that the tryptophan residues in gramicidin A′ are localized in a motionally restricted region of the membrane.

It is known that tryptophan has two overlapping $S_0 \rightarrow S_1$ electronic transitions (^1L_a and ^1L_b) which are almost perpendicular to each other (Weber, 1960a; Song & Kurtin, 1969; Yamamoto & Tanaka, 1972; Eftink, 1991). Both $S_0 \rightarrow {}^1L_a$ and $S_0 \rightarrow {}^1L_b$ transitions occur in the 260–300-nm range. In nonpolar solvents, ^1L_a has higher energy than ^1L_b. However, in polar solvents, the energy level of ^1L_a is lowered, making it the lowest energy state. This inversion is believed to occur because the ^1L_a transition has a higher dipole moment (as it is directed through the ring–NH group), and can have dipole–dipole interactions with polar solvent molecules. Whether ^1L_a or ^1L_b is the lowest S_1 state, equilibration between these two states is believed to be very fast (of the order of 10^{-12} s), so that only emission from the lower S_1 state is observed (Ruggiero *et al.*, 1990). In a motionally restricted polar environment, absorption at the red edge photoselects the lowest energy S_1 (^1L_a in this case), and thus the polarization is high since only depolarization due to small angular differences between the absorption and emission transition moments and solvent reorientation, if any, occurs. Excitation at the shorter wavelengths, however, populates both ^1L_a and ^1L_b states. Equilibration between these two states produces a depolarization due to the approximately 90° angular difference between ^1L_a and ^1L_b moments. Thus, near 290 nm, there is a sharp dip in polarization due to maximal absorption by the ^1L_b state. Figure 2 shows such a characteristic dip around 290 nm in the excitation polarization spectrum of gramicidin A′. Thus, the sharp increase in polarization toward the red edge of the absorption band is probably because the extent of depolarization in gramicidin is reduced at the red edge not only due to a decreased rotational rate of the fluorophore in the solvent-relaxed state but also due to photoselection of the predominantly ^1L_a transition, which in turn reduces the contribution to depolarization because of $^1L_b \rightarrow {}^1L_a$ equilibration.

The photoselection of the ^1L_a state toward the red edge could also account for the rather sharp change in the emission maximum with excitation wavelength for gramicidin A′ in membranes, as is apparent from Figure 1. The excited-state interactions with the solvent dipoles will be stronger for the ^1L_a state because of its higher dipole moment. This would enhance the extent of red shift in the emission maximum at higher excitation wavelengths.

Table 1: Lifetimes of Tryptophans in Gramicidin Channels as a Function of Excitation Wavelength[a]

excitation wavelength (nm)	α_1	τ_1 (ns)	f_1	α_2	τ_2 (ns)	f_2	χ^2
294	0.89	0.8	0.64	0.11	3.6	0.36	1.7
297	0.90	0.6	0.64	0.10	3.0	0.36	1.2
305	0.95	0.4	0.72	0.05	3.0	0.28	1.9
313	0.98	0.4	0.83	0.02	4.0	0.17	1.9
316	0.99	0.4	0.91	0.01	3.9	0.09	1.6

[a] Emission wavelength 340 nm.

As has been discussed earlier, the origin of the red edge effect lies in differential extents of solvent reorientation around the excited-state fluorophore, with each excitation wavelength selectively exciting a different average population of fluorophores. Since the fluorescence lifetime is known to be sensitive to excited-state interactions, differential extents of solvent relaxation around a given fluorophore could be expected to give rise to a difference in its lifetime. Also, gramicidin being a multi-tryptophan peptide, any steady-state fluorescence data will represent a statistical average of the contributions from individual tryptophans, and, hence, such steady-state information is only indicative of the average environment experienced by the tryptophans. Although time-resolved fluorescence studies do not always provide information regarding each individual fluorescing species, they are sensitive enough to resolve two or more different environments around the same fluorophore.

Table 1 shows the lifetimes of the tryptophan residues of gramicidin channels in DOPC vesicles as a function of excitation wavelength, keeping the emission wavelength fixed at 340 nm. As can be seen from Table 1, when gramicidin A′ in DOPC vesicles is excited at 297 nm, the decay fits a biexponential function, with the major lifetime component (preexponential factor 0.90) having a very short lifetime of 0.6 ns and the minor component (preexponential factor 0.10) having a relatively longer lifetime of 3.0 ns. The decay profile with its biexponential fitting and the various statistical parameters used to check the goodness of the fit are shown in Figure 3.

When the excitation wavelength was gradually shifted from 294 to 316 nm, *i.e.*, toward the red edge of the absorption band, keeping the emission wavelength constant at 340 nm (see Table 1), it was found that the individual lifetimes did not change significantly. Interestingly, the preexponential factor for the short-lifetime component as well as the fractional intensity associated with it increased steadily, with a concomitant reduction in the above parameters for the relatively long-lifetime component. The mean fluorescence lifetimes of the tryptophan residues of gramicidin were calculated using eq 3 and are plotted as a function of excitation wavelength in Figure 4. As shown in this figure, there is a steady decrease (~61%) in the mean lifetime with increasing excitation wavelength from 294 to 316 nm. Such a marked shortening of lifetime at the red edge of the absorption band is indicative of slow solvent reorientation around the excited-state fluorophore (Castelli & Forster, 1973; Valeur & Weber, 1978). The emission wavelength was set at 340 nm in order to avoid scattering artifacts at longer excitation wavelengths.

Table 2 shows the lifetimes of tryptophan residues of gramicidin channels in DOPC vesicles as a function of the

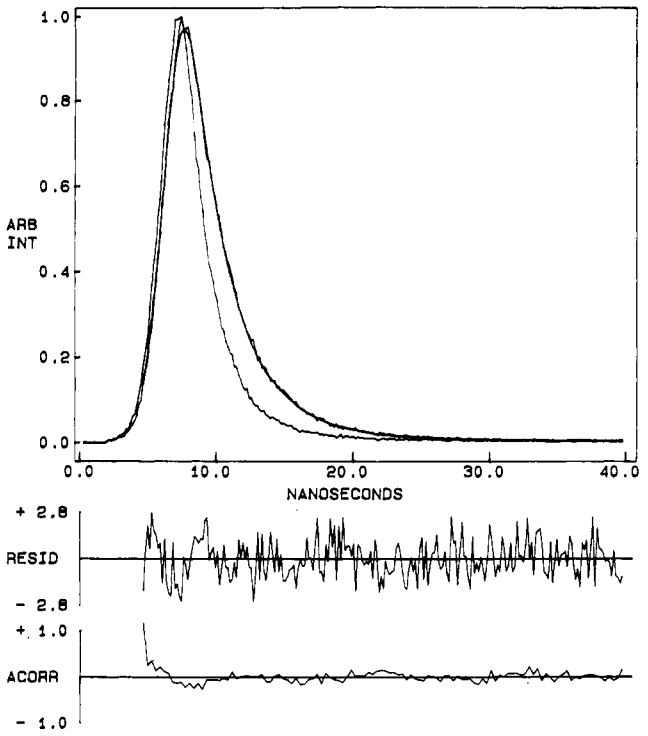

FIGURE 3: Time-resolved fluorescence intensity decay of gramicidin A′ in ULVs of DOPC. Excitation was at 297 nm, which corresponds to a peak in the spectral output of the nitrogen lamp. Emission was monitored at 340 nm. The sharp peak on the left is the lamp profile. The relatively broad peak on the right is the decay profile, fitted to a biexponential function. The two lower plots show the weighted residuals and the autocorrelation function of the weighted residuals. Fluorophore to lipid ratio was 1:100 (mol/mol). See Materials and Methods for other details.

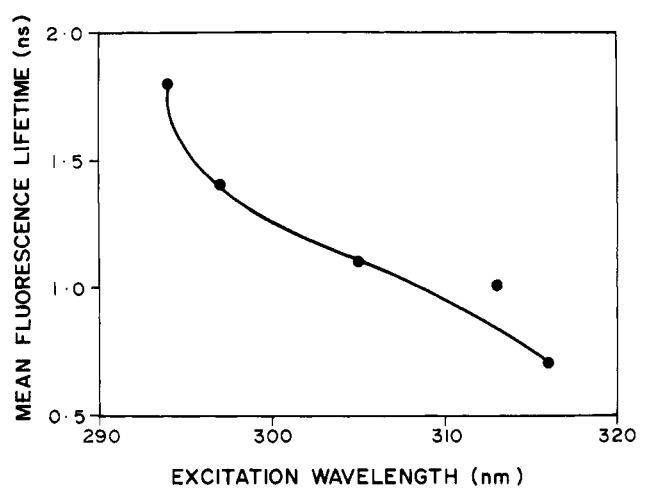

FIGURE 4: Mean fluorescence lifetime of gramicidin A′ in DOPC vesicles as a function of excitation wavelength. Emission wavelength was kept constant at 340 nm. Mean lifetimes were calculated from Table 1 using eq 3. Fluorophore to lipid ratio was 1:100 (mol/mol). See Materials and Methods for other details.

emission wavelength, keeping the excitation wavelength constant at 297 nm. All decays corresponding to different emission wavelengths could be fitted to biexponential functions. As can be seen from the table, the tryptophan residues exhibit two lifetimes at all the emission wavelengths studied, the major component (preexponential factor ~0.9) having a lifetime of 0.5–1.6 ns and the minor component (preexponential factor ~0.1) having a lifetime of 2.6–8.8 ns. As the emission wavelength is gradually shifted from 330 to 380 nm, *i.e.*, toward the red edge of the spectrum, the preexponential factors and fractional intensities remain essentially the same, but both lifetime components increase steadily with increasing emission

Table 2: Lifetimes of Tryptophans in Gramicidin Channels as a Function of Emission Wavelength[a]

emission wavelength (nm)	α_1	τ_1 (ns)	f_1	α_2	τ_2 (ns)	f_2	χ^2
330	0.93	0.5	0.72	0.07	2.6	0.28	1.6
340	0.90	0.6	0.64	0.10	3.0	0.36	1.2
350	0.89	0.9	0.68	0.11	3.4	0.32	1.8
360	0.94	1.3	0.80	0.06	5.2	0.20	1.4
370	0.95	1.4	0.81	0.05	6.2	0.19	1.8
380	0.96	1.6	0.81	0.04	8.8	0.19	1.5

[b] Excitation wavelength 297 nm.

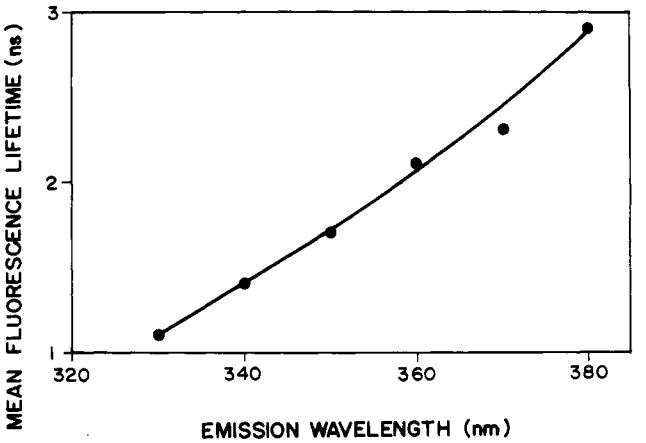

FIGURE 5: Mean fluorescence lifetime of gramicidin A′ in DOPC vesicles as a function of emission wavelength. Excitation wavelength used was 297 nm. Mean lifetimes were calculated from Table 2 using eq 3. All other conditions are as in Figure 4.

wavelength. The mean lifetimes, calculated using eq 3, are plotted as a function of emission wavelength in Figure 5. The mean lifetime increases by ~62% with increasing emission wavelength from 330 to 380 nm. Such an observation has been reported previously for fluorophores in environments of restricted mobility (Easter *et al.*, 1976; Lakowicz & Cherek, 1980; Matayoshi & Kleinfeld, 1981; Lakowicz *et al.*, 1983). Such increasing lifetimes across the emission spectrum may be interpreted in terms of solvent reorientation around the excited-state fluorophore as follows. Observation at the short emission wavelengths selects for predominantly unrelaxed fluorophores. Their lifetimes are shorter because this population is decaying both at the rate of fluorescence emission at the given excitation wavelength and by decay to longer (unobserved) wavelengths. In contrast, observation at the long-wavelength (red) edge of the emission selects for the more relaxed fluorophores, which have spent enough time in the excited state in order to allow increasingly larger extents of solvent reorientation.

Such longer-lived fluorophores, which are also those which emit at higher wavelengths, should, in principle, have more time to rotate in the excited state, giving rise to lower polarization. Figure 6 shows the variation in the steady-state polarization of tryptophan residues of gramicidin in DOPC vesicles and in methanol, as a function of wavelength across its emission spectrum. As seen from the figure, while polarization values do not show any significant variation over the entire emission range in methanol, there is a considerable decrease in polarization with increasing emission wavelength in the case of membrane-bound gramicidin. The lowest polarization is observed toward the red edge where the relaxed emission predominates. Similar observations have previously been reported for other membrane-bound fluorophores (Matayoshi & Kleinfeld, 1981; Lakowicz *et al.*, 1983; Sommer *et al.*, 1990; Chattopadhyay & Mukherjee, 1993; Chattopadhyay & Rukmini, 1993).

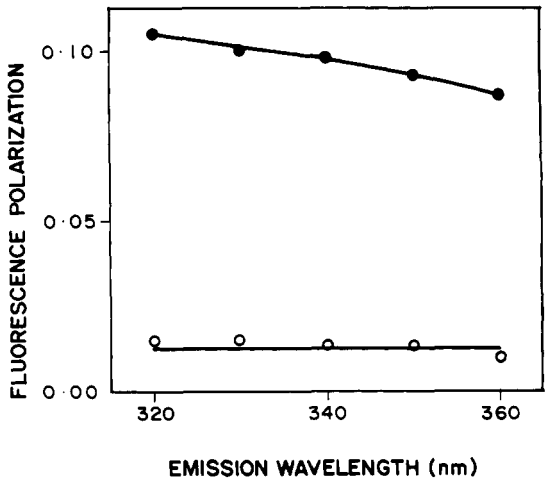

FIGURE 6: Fluorescence polarization of gramicidin A′ as a function of emission wavelength in methanol (○) and in DOPC vesicles (●). The excitation wavelength was 280 nm. Fluorophore to lipid ratio was 1:100 (mol/mol) in DOPC vesicles. Concentration of gramicidin A′ in methanol was 4.3 μM. See Materials and Methods for other details.

Figure 7 shows the time-resolved emission spectra (TRES) of membrane-bound gramicidin channels at early and late time points. Two distinct emission peaks were observed: one around 320 nm and the other around 340 nm. As is apparent from the figure, the peak at 320 nm decays extremely fast, corresponding to a very short lifetime. The long-wavelength (340 nm) peak, on the other hand, decays much more slowly, indicating that it has a relatively long lifetime. Figure 7a shows a clear rise time for the 340-nm peak; *i.e*, the intensity of the peak increases for a while after the lamp pulse, only after which it starts decaying. Such a rise time for a time-resolved fluorescence peak is clearly indicative of solvent dipole reorientation around the excited-state fluorophores (Easter *et al.*, 1976; Lakowicz, 1983; Sommer *et al.*, 1990).

DISCUSSION

Tryptophan residues in gramicidin channels are believed to be crucial for maintaining the structure and function of the channel (Hu *et al.*, 1993). The importance of the tryptophans has been demonstrated by the observation that the cation conductivity of the channel decreases upon substitution of one or all of the tryptophan residues by phenylalanine, tyrosine, or naphthylalanine (Bamberg *et al.*, 1976; Heitz *et al.*, 1982; Prasad *et al.*, 1983; Trudelle & Heitz, 1987; Daumas *et al.*, 1989; Becker *et al.*, 1991; Fonseca *et al.*, 1992), and also upon ultraviolet irradiation or chemical modification of the tryptophan rings (Busath & Waldbilling, 1983; Jones *et al.*, 1986; Strassle *et al.*, 1989). In fact, it has been proposed that the tryptophan dipoles facilitate ion entry into the gramicidin channels by aligning with the lipid head group electric field and producing a contrary field that reduces the surface potential of the membrane, which under normal circumstances inhibits ion entry into the bilayer (Busath, 1993).

As stated earlier, the preference for the $\beta^{6.3}$-helical conformation of the gramicidin channel in the membrane environment has been suggested to be due to a preferred orientation of the tryptophans near the lipid–water interface. This preferred localization, in turn, has been ascribed to the ability of the tryptophan –NH groups to participate in hydrogen bond formation with acceptors near the lipid head groups, one of the strongest candidates for such acceptors being the lipid carbonyls (O'Connell *et al.*, 1990; Ippolito *et al.*, 1990; Becker *et al.*, 1991; Scarlata, 1991; Killian, 1992). Also, being localized at the membrane interface, hydrogen bond formation with the surrounding interfacial water molecules is a distinct possibility. Such hydrogen bonding could play an important role in stabilizing the channel in the lipid bilayer and in modulating the hydration of cations passing through the channel. The role of hydration at the peptide–lipid interface of gramicidin channels has recently been addressed by Ho and Stubbs (1992). These authors point out that in the case of membrane proteins, the level of hydration at the protein–lipid interface could have modulatory effects on the structure and function of the protein.

A close look at the $\beta^{6.3}$ helix reveals that for any residue in the primary sequence (residue *i*), the adjacent residue (residue *i* + 1) and the seventh residue from it (residue *i* + 6) are close together in space. An interaction is therefore

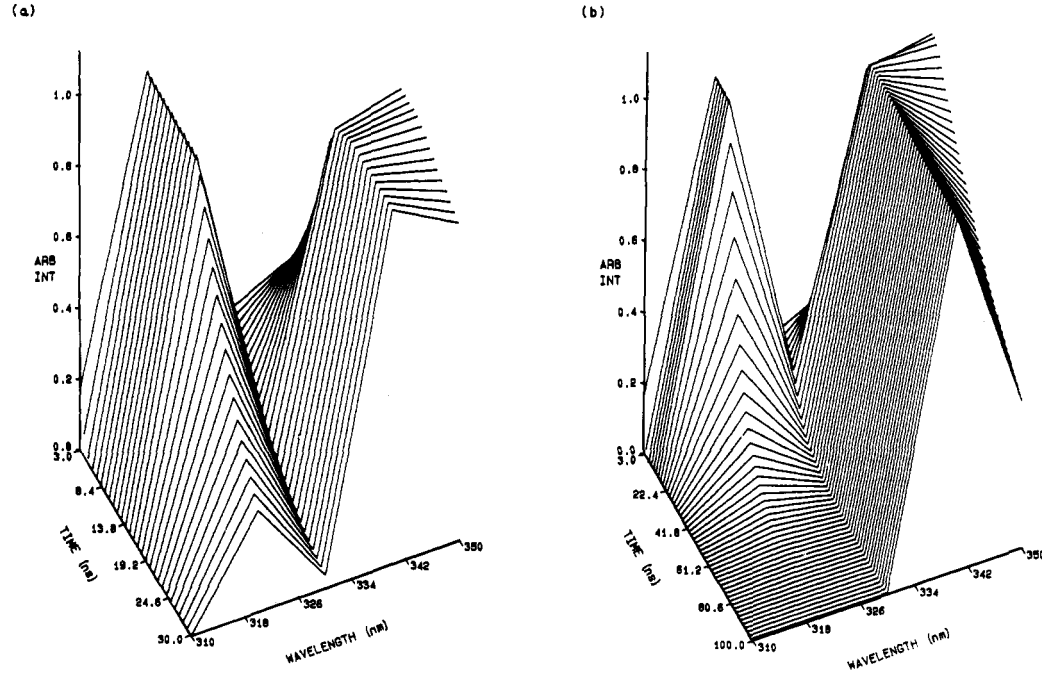

FIGURE 7: Time-resolved emission spectra (TRES) of gramicidin A′ in DOPC vesicles at (a) early time points and (b) late time points. Excitation wavelength used was 297 nm. The reduced χ^2 ratio, the weighted residuals, and the autocorrelation function of the weighted residuals were checked at each emission wavelength monitored. See text for other details.

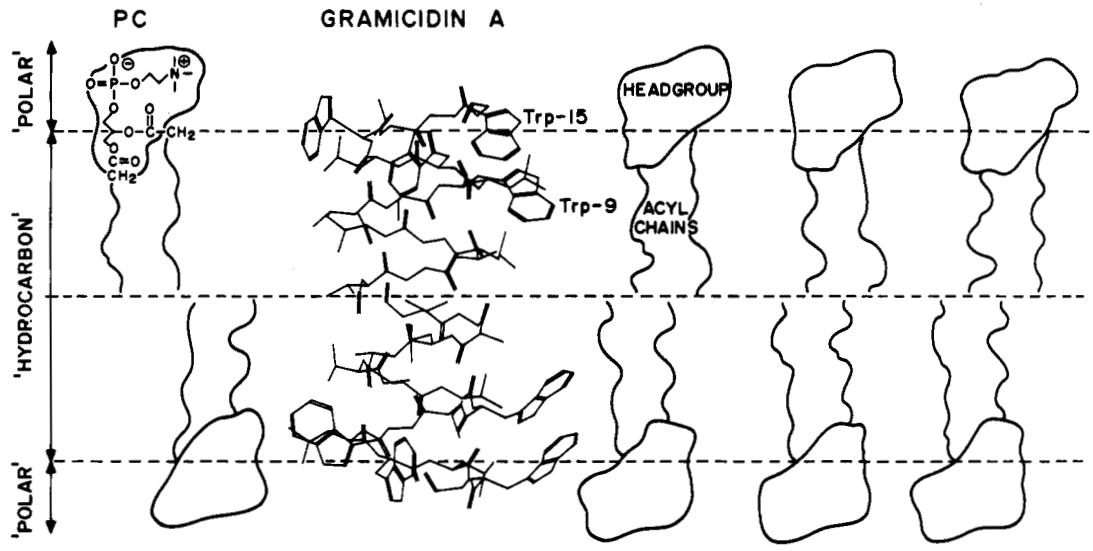

FIGURE 8: Schematic diagram of the membrane bilayer showing the orientation and location of gramicidin A. The molecular model of the gramicidin channel is adapted from Wallace (1990). The coordinates of the gramicidin molecule, as determined by Roux and Karplus (1988), are those obtained after energy minimization of the model proposed by Urry *et al.* (1971). The tryptophans (9 and 15) which could be involved in aromatic–aromatic interaction are shown (see text). The middle line indicates the center of the bilayer.

possible between Trp-9 and Trp-15 due to their close proximity. Data from fluorescence, circular dichroism, and solid-state NMR spectroscopy suggest that tryptophans-9 and -15 could be involved in a specific aromatic–aromatic interaction which has been previously interpreted as a stacking interaction (Cavatorta *et al.*, 1982; Masotti *et al.*, 1986; Wallace, 1986; Scarlata, 1988, 1991; Ketchem *et al.*, 1993). Interactions among such closely spaced aromatic amino acids have previously been implicated as a possible mechanism of protein structure stabilization (Burley & Petsko, 1985).

Such interactions among the closely localized tryptophan residues and the bulky nature of their side chains, in addition to their proposed hydrogen bonding with the lipid carbonyls (or interfacial water), may be expected to reduce the conformational flexibility and the range of motions of the side chains. This is consistent with the reported correlation times ($\sim 2 \times 10^{-7}$ s) of gramicidin tryptophans as determined by deuterium nuclear magnetic resonance (Macdonald & Seelig, 1988). In this paper, we have shown that the tryptophan environments in membrane-bound gramicidin channels are indeed motionally restricted, as seen by a shift in the maximum of fluorescence emission as a function of excitation wavelength (REES), and also by a dependence of the fluorescence polarization as well as lifetimes on both excitation and emission wavelengths.

Further, our studies show that the fluorescence decays of the tryptophan residues of membrane-bound gramicidin A′ exhibit a biexponential character at all the excitation and emission wavelengths studied. One of these is a very short-lifetime component (0.4–1.6 ns) with a relatively large contribution to the total fluorescence (fractional intensity ~0.6–0.9), and the other is a longer lifetime component (2.6–8.8 ns) with a smaller fractional intensity (~0.1–0.4). The time-resolved emission spectra of membrane-bound gramicidin A′ are consistent with these lifetime data. Two distinct emission peaks are observed: one at ~320 nm and the other at ~340 nm. As is apparent from Figure 7, the peak at 320 nm decays extremely fast; *i.e.*, it has a very short lifetime. The long-wavelength peak, on the other hand, decays much more slowly; *i.e.*, it has a relatively long lifetime.

The resolution of the emission maximum into two different peaks on the time axis may have its origin either in the ground-state heterogeneity or in an excited-state interaction (Badea & Brand, 1979). Ground-state heterogeneity arising either due to the presence of gramicidin in the bulk aqueous phase or due to the presence of gramicidin monomers in the membrane can be ruled out as follows. No contribution can come from gramicidin monomer in water, because gramicidin, being very hydrophobic, has extremely low solubility in aqueous solutions ($\sim 5 \times 10^{-7}$ M) (Kemp *et al.*, 1972). Also, Veatch *et al.* (1975) calculated the dimerization constant of gramicidin A in DOPC black lipid membranes to be $\sim 2 \times 10^{13}$ mol^{-1} cm^2. This means that at the peptide concentration generally employed for spectroscopic experiments in lipid vesicles, the fraction of monomers is negligible. In addition, heterogeneity because of minor components in gramicidin A′ (gramicidins B and C) is eliminated since it has been reported that the emission spectra and lifetimes of pure gramicidin A in model membranes are identical with those obtained for the commercially available gramicidin A′ samples (Camaleno-Delango *et al.*, 1990).

Since the two lifetimes obtained by us at all excitation and emission wavelengths are drastically different from each other and, also, two clear peaks are seen in the TRES plot, we are tempted to conclude that the tryptophan residues of gramicidin A′ are in two distinct environments in the membrane. We propose that the short-lifetime component in the fluorescence decays and also the fast-decaying TRES peak correspond to an interacting tryptophan pair. This pair could be tryptophans-9 and -15 because of their close proximity in a $\beta^{6.3}$-helical configuration [as also suggested by Masotti *et al.* (1986)]. The presence of such an interacting tryptophan pair (9 and 15) has previously been suggested from structural studies of gramicidin channels in lipid bilayers using solid-state NMR spectroscopy (Hu *et al.*, 1993; Ketchem *et al.*, 1993). The longer wavelength (340 nm) TRES peak having a longer lifetime, as well as the long-lifetime component in the fluorescence decays, may therefore represent the average environment experienced by the remaining two tryptophans, namely, Trp-11 and Trp-13. Since this component has a longer lifetime, the solvent dipolar relaxation can be clearly seen as a rise time for this peak; *i.e.*, the intensity of this peak increases for a while after the lamp pulse, only after which it starts decaying. Such a rise time for a time-resolved fluorescence peak strongly suggests slow solvent dipole reorientation around the excited-state fluorophores (Easter *et al.*, 1976; Lakowicz, 1983).

The above interpretation of our time-resolved fluorescence data is not in complete agreement with the model of the gramicidin channel in SDS micelles derived from NMR spectroscopy (Arseniev *et al.*, 1986). However, the precise configuration of the gramicidin channel in the micellar environment may differ from that in the bilayer because of (i) the intrinsic difference in the radius of curvature (the micellar surface has a much larger curvature than the bilayer) and (ii) the important interfacial characteristics of the phospholipid bilayer, which is crucial for the appropriate orientation and localization of tryptophans in this region (as discussed earlier) and is lacking in the SDS micelles. It is of interest to note here that although the short-lifetime component has a high fractional intensity, its contribution to the steady-state spectrum will still be very low because of its very fast decay.

In conclusion, our studies suggest that the tryptophan residues of gramicidin are present in motionally restricted regions of the membrane and can be grouped into at least two classes experiencing very different microenvironments. According to our interpretation, one of these classes could be tryptophans-9 and -15, which are proposed to participate in aromatic–aromatic interaction, and the other class could be the average environment experienced by tryptophans-11 and -13, which shows clear evidence of slow solvent reorientation in the fluorescence time scale. Such evidence of motional restriction experienced by the tryptophans in the membrane-bound gramicidin channel, in addition to the evidence presented for the slow rate of solvent dipole reorientation, is clearly indicative of the localization of these tryptophans at the lipid–water interface of the membrane (see Figure 8). This region of the membrane is characterized by unique motional and dielectric characteristics (Ashcroft *et al.*, 1981; Stubbs *et al.*, 1985; Perochon *et al.*, 1992; Slater *et al.*, 1993) different from the bulk aqueous phase and the more isotropic hydrocarbon-like deeper regions of the membrane. This specific region of the membrane is also known to participate in intermolecular charge interactions (Yeagle, 1987) and hydrogen bonding through the polar head group (Boggs, 1987; Shin *et al.*, 1991). These structural features which slow down the rate of solvent reorientation have previously been recognized as typical features of solvents giving rise to significant red edge effects (Itoh & Azumi, 1975).

In more general terms, our results also suggest that caution should be exercised while interpreting emission characteristics and fluorescence lifetimes of the tryptophan residues in proteins and peptides. The excitation maxima of tryptophan and tyrosine residues are very close (280 and 275 nm, respectively). In order to selectively excite tryptophan residues, therefore, proteins are often excited at 295 nm (red edge of the tryptophan absorption band, having minimal interference from the tyrosine excitation), instead of 280 nm, which is the mean excitation wavelength for tryptophan (Teale, 1960; Longworth, 1971). If all the tryptophan residues of the protein are well exposed to the solvent, it is unlikely that the red edge effect will be operative in fluid solutions. In such a case, excitation at 295 nm will not introduce any artifacts in either the emission maximum or the lifetime of the tryptophan residues. However, tryptophans in polar yet restricted environments (*e.g.*, buried or membrane-bound tryptophans having water or other amino acid side chains or lipid carbonyl dipoles in its immediate vicinity) may well be subject to this effect. Under such conditions, excitation of the protein at 295 nm could introduce a red shift in its emission maximum, as well as a reduction in its mean lifetime, both of which may be incorrectly interpreted as tryptophan residues being more exposed to the bulk aqueous phase than they really are. Thus, it is important to consider the choice of wavelengths in such experiments.

ACKNOWLEDGMENT

We thank Y. S. S. V. Prasad and G. G. Kingi for technical help and Drs. D. Chatterji and R. Nagaraj for helpful discussions. The Photon Technology International LS-100 luminescence spectrophotometer used in this study was purchased from a grant awarded by the Department of Science and Technology, Government of India.

REFERENCES

Andersen, O. S. (1984) *Annu. Rev. Physiol. 46*, 531–548.
Andersen, O. S., & Koeppe, R. E. (1992) *Physiol. Rev. (Suppl.) 72*, S89–S158.
Andersen, O. S., Sawyer, D. B., & Koeppe, R. E. (1992) in *Biomembrane Structure & Function: The State of the Art* (Gaber, B. P., & Easwaran, K. R. K., Eds.) pp 227–244, Adenine Press, Schenectady, NY.
Arseniev, A. S., Lomize, A. L., Barsukov, I. L., & Bystrov, V. F. (1986) *Biol. Membr. 3*, 1077–1104.
Ashcroft, R. G., Coster, H. G. L., & Smith, J. R. (1981) *Biochim. Biophys. Acta 643*, 191–204.
Badea, M. G., & Brand, L. (1979) *Methods Enzymol. 61*, 378–425.
Bamberg, E., Noda, K., Gross, E., & Lauger, P. (1976) *Biochim. Biophys. Acta 419*, 223–228.
Bano, M. C., Braco, L., & Abad, C. (1992) *Biophys. J. 63*, 70–77.
Becker, M. D., Greathouse, D. V., Koeppe, R. E., & Andersen, O. S. (1991) *Biochemistry 30*, 8830–8839.
Bevington, P. R. (1969) *Data Reduction and Error Analysis for the Physical Sciences*, McGraw-Hill, New York.
Boggs, J. M. (1987) *Biochim. Biophys. Acta 906*, 353–404.
Boni, L. T., Connolly, A. J., & Kleinfeld, A. M. (1986) *Biophys. J. 49*, 122–123.
Burley, S. K., & Petsko, G. A. (1985) *Science 229*, 23–28.
Busath, D. D. (1993) *Annu. Rev. Physiol. 55*, 473–501.
Busath, D. D., & Waldbilling, R. C. (1983) *Biochim. Biophys. Acta 736*, 28–38.
Camaleno-Delango, J.-M., Zhao, X. K., & Fendler, J. H. (1990) *Can. J. Chem. 68*, 888–896.
Castelli, F., & Forster, L. S. (1973) *J. Am. Chem. Soc. 95*, 7223–7226.
Cavatorta, P., Spisni, A., Casali, E., Lindner, L., Masotti, L., & Urry, D. W. (1982) *Biochim. Biophys. Acta 689*, 113–120.
Chapman, D., Cornell, B. A., Eliasz, A. W., & Perry, A. (1977) *J. Mol. Biol. 113*, 517–538.
Chattopadhyay, A. (1990) *Chem. Phys. Lipids 53*, 1–15.
Chattopadhyay, A. (1991) *Biophys. J. 59*, 191a (Abstr.).
Chattopadhyay, A., & McNamee, M. G. (1991) *Biochemistry 30*, 7159–7164.
Chattopadhyay, A., & Mukherjee, S. (1993) *Biochemistry 32*, 3804–3811.
Chattopadhyay, A., & Rukmini, R. (1993) *FEBS Lett. 335*, 341–344.
Chen, R. F., & Bowman, R. L. (1965) *Science 147*, 729–732.
Cornell, B. (1987) *J. Bioenerg. Biomembr. 19*, 655–676.
Daumas, P., Heitz, F., Ranjalahy-Rasoloarijao, L., & Lazaro, R. (1989) *Biochimie 71*, 77–81.
Demchenko, A. P. (1982) *Biophys. Chem. 15*, 101–109.
Demchenko, A. P. (1988) *Trends Biochem. Sci. 13*, 374–377.
Dittmer, J. C., & Lester, R. L. (1964) *J. Lipid Res. 5*, 126–127.
Durbin, J., & Watson, G. S. (1950) *Biometrika 37*, 409–428.
Easter, J. H., DeToma, R. P., & Brand, L. (1976) *Biophys. J. 16*, 571–583.
Eftink, M. R. (1991) *Methods Biochem. Anal. 35*, 127–205.
Feigenson, G. W., Meers, P. R., & Kingsley, P. B. (1977) *Biochim. Biophys. Acta 471*, 487–491.
Finkelstein, A., & Andersen, O. S. (1981) *J. Membr. Biol. 59*, 155–171.

Fonseca, V., Daumas, P., Ranjalahy-Rasoloarijao, L., Heitz, F., Lazaro, R., Trudelle, Y., & Andersen, O. S. (1992) *Biochemistry 31*, 5340–5350.
Galley, W. C., & Purkey, R. M. (1970) *Proc. Natl. Acad. Sci. U.S.A. 67*, 1116–1121.
Grinvald, A., & Steinberg, I. Z. (1974) *Anal. Biochem. 59*, 583–598.
Guy, H. R. (1988) *Curr. Top. Membr. Transp. 33*, 289–308.
Haigh, E. A., Thulborn, K. R., & Sawyer, W. H. (1979) *Biochemistry 18*, 3525–3532.
Hamburg, M. (1985) *Basic Statistics*, Harcourt Brace Jovanovich, New York.
Heitz, F., Spach, G., & Trudelle, Y. (1982) *Biophys. J. 40*, 87–89.
Hladky, S. B., & Haydon, D. A. (1972) *Biochim. Biophys. Acta 274*, 294–312.
Ho, C., & Stubbs, C. D. (1992) *Biophys. J. 63*, 897–902.
Hu, W., Lee, K.-C., & Cross, T. A. (1993) *Biochemistry 32*, 7035–7047.
Ippolito, J. A., Alexander, R. S., & Christianson, D. W. (1990) *J. Mol. Biol. 215*, 457–471.
Itoh, K.-I., & Azumi, T. (1975) *J. Chem. Phys. 62*, 3431–3438.
Jacobs, R. E., & White, S. H. (1989) *Biochemistry 28*, 3421–3437.
Jones, D., Hayon, E., & Busath, D. (1986) *Biochim. Biophys. Acta 861*, 62–66.
Kemp, G., Jacobson, K. A., & Wenner, C. E. (1972) *Biochim. Biophys. Acta 255*, 493–501.
Ketchem, R. R., Hu, W., & Cross, T. A. (1993) *Science 261*, 1457–1460.
Killian, J. A. (1992) *Biochim. Biophys. Acta 1113*, 391–425.
Killian, J. A., Prasad, K. U., Hains, D., & Urry, D. W. (1988) *Biochemistry 27*, 4848–4855.
Lakowicz, J. R. (1983) *Principles of Fluorescence Spectroscopy*, Plenum Press, New York.
Lakowicz, J. R. (1984) *Biophys. Chem. 19*, 13–23.
Lakowicz, J. R., & Cherek, H. (1980) *J. Biol. Chem. 255*, 831–834.
Lakowicz, J. R., & Keating-Nakamoto, S. (1984) *Biochemistry 23*, 3013–3021.
Lakowicz, J. R., Bevan, D. R., Maliwal, B. P., Cherek, H., & Balter, A. (1983) *Biochemistry 22*, 5714–5722.
Lampert, R. A., Chewter, L. A., Phillips, D., O'Connor, D. V., Roberts, A. J., & Meech, S. R. (1983) *Anal. Chem. 55*, 68–73.
LoGrasso, P. V., Moll, F., & Cross, T. A. (1988) *Biophys. J. 54*, 259–267.
Longworth, J. W. (1971) in *Excited States of Proteins and Nucleic Acids* (Steiner, R. F., & Weinryb, I., Eds.) pp 319–484, Plenum Press, New York.
Macdonald, P. M., & Seelig, J. (1988) *Biochemistry 27*, 2357–2364.
Masotti, L., Cavatorta, P., Sartor, G., Casali, E., & Szabo, A. G. (1986) *Biochim. Biophys. Acta 862*, 265–272.
Matayoshi, E. D., & Kleinfeld, A. M. (1981) *Biophys. J. 35*, 215–235.
McClare, C. W. F. (1971) *Anal. Biochem. 39*, 527–530.
Meers, P. (1990) *Biochemistry 29*, 3325–3330.
Meulendijks, G. H. W. M., Sonderkamp, T., Dubois, J. E., Nielen, R. J., Kremers, J. A., & Buck, H. M. (1989) *Biochim. Biophys. Acta 979*, 321–330.
Michel, H., & Deisenhofer, J. (1990) *Curr. Top. Membr. Transp. 36*, 53–69.
O'Connell, A. M., Koeppe, R. E., & Andersen, O. S. (1990) *Science 250*, 1256–1259.
O'Connor, D. V., & Phillips, D. (1984) in *Time-Correlated Single Photon Counting*, pp 180–189, Academic Press, London.
Perochon, E., Lopez, A., & Tocanne, J. F. (1992) *Biochemistry 31*, 7672–7682.
Prasad, K. U., Trapane, T. L., Busath, D., Szabo, G., & Urry, D. W. (1983) *Int. J. Pept. Protein Res. 22*, 341–347.
Ramachandran, G. N., & Chandrasekaran, R. (1972) *Indian J. Biochem. Biophys. 9*, 1–11.
Rice, D., & Oldfield, E. (1979) *Biochemistry 18*, 3272–3279.
Rinehart, K. L., Cook, J. C., Meng, H., Olson, K. L., & Pandey, R. C. (1977) *Nature 269*, 832–833.
Roux, B., & Karplus, M. (1988) *Biophys. J. 53*, 297–309.
Ruggiero, A. J., Todd, D. C., & Fleming, G. R. (1990) *J. Am. Chem. Soc. 112*, 1003–1014.
Sarges, R., & Witkop, B. (1965) *J. Am. Chem. Soc. 87*, 2011–2020.
Scarlata, S. F. (1988) *Biophys. J. 54*, 1149–1157.
Scarlata, S. F. (1991) *Biochemistry 30*, 9853–9859.
Schiffer, M., Chang, C.-H., & Stevens, F. J. (1992) *Protein Eng. 5*, 213–214.
Segrest, J. P., & Feldmann, R. J. (1974) *J. Mol. Biol. 87*, 853–858.
Shin, T.-B., Leventis, R., & Silvius, J. R. (1991) *Biochemistry 30*, 7491–7497.
Slater, S. J., Ho, C., Taddeo, F. J., Kelly, M. B., & Stubbs, C. D. (1993) *Biochemistry 32*, 3714–3721.
Sommer, A., Paltauf, F., & Hermetter, A. (1990) *Biochemistry 29*, 11134–11140.
Song, P.-S., & Kurtin, W. E. (1969) *J. Am. Chem. Soc. 91*, 4892–4906.
Strassle, M., Stark, G., Wilhelm, M., Daumas, P., Heitz, F., & Lazaro, R. (1989) *Biochim. Biophys. Acta 980*, 305–314.
Stubbs, C. D., Meech, S. R., Lee, A. G., & Phillips, D. (1985) *Biochim. Biophys. Acta 815*, 351–360.
Susi, H., Sampugna, J., Hampson, J. W., & Ard, J. S. (1979) *Biochemistry 18*, 297–301.
Teale, F. W. J. (1960) *Biochem. J. 76*, 381–388.
Trudelle, Y., & Heitz, F. (1987) *Int. J. Pept. Protein Res. 30*, 163–169.
Urry, D. W. (1971) *Proc. Natl. Acad. Sci. U.S.A. 68*, 672–676.
Urry, D. W., Goodall, M. C., Glickson, J. D., & Mayers, D. F. (1971) *Proc. Natl. Acad. Sci. U.S.A. 68*, 1907–1911.
Valeur, B., & Weber, G. (1977) *Chem. Phys. Lett. 45*, 140–144.
Valeur, B., & Weber, G. (1978) *J. Chem. Phys. 69*, 2393–2400.
Veatch, W. R., & Blout, E. R. (1974) *Biochemistry 13*, 5257–5264.
Veatch, W. R., Mathies, R., Eisenberg, M., & Stryer, L. (1975) *J. Mol. Biol. 99*, 75–92.
Wallace, B. A. (1986) *Biophys. J. 49*, 295–306.
Wallace, B. A. (1990) *Annu. Rev. Biophys. Biophys. Chem. 19*, 125–157.
Weber, G. (1960a) *Biochem. J. 75*, 335–345.
Weber, G. (1960b) *Biochem. J. 75*, 345–352.
Weidekamm, E., Bamberg, E., Brdiczka, D., Wildermuth, G., Macco, F., Lehmann, W., & Weber, R. (1977) *Biochim. Biophys. Acta 464*, 442–447.
Weiss, M. S., Abele, U., Weckesser, J., Welte, W., Schiltz, E., & Schultz, G. E. (1991) *Science 254*, 1627–1630.
Yamamoto, Y., & Tanaka, J. (1972) *Bull. Chem. Soc. Jpn. 45*, 1362–1366.
Yeagle, P. (1987) *The Membranes of Cells*, pp 89–90, Academic Press, Orlando, FL.